Simultaneous quantum-state measurements using array detection

A. M. Dawes and M. Beck*

Department of Physics, Whitman College, Walla Walla, Washington 99362
(Received 10 November 2000; published 19 March 2001)

We have simultaneously measured the quantum states of two different spatial modes of the same optical beam by performing quantum-state tomography with an array detector. Both modes are well described by coherent states, but the projection of the signal onto the local oscillator mode contains a mean of 0.09 photons, while a more complicated mode has a mean of 4.3 photons. This demonstrates that for this particular mode the effective detection efficiency when using array detection is over 40 times greater than when using single detectors.

Array detectors represent a practical means of making simultaneous measurements of optical fields at many different spatial locations. Present state-of-the-art charge-coupled device (CCD) arrays have specifications that are as good as, or better than, stand alone single detectors: quantum efficiencies of over 90%, dark count rates of less than one electron per pixel per hour, and electronic read noise approaching one electron per pixel. A few theoretical treatments have discussed using the unique properties of arrays to make quantum measurements that are difficult, or impossible, with standard single detectors [1–3]. A number of interesting quantum-mechanical effects that appear in the spatial distribution of optical fields have been discussed [4–6], but experiments that explore these effects have so far not taken advantage of the benefits afforded by array detectors [7,8].

Here we present the results of an experiment that uses array detection to measure quantum states of an optical beam. This experiment implements a proposal recently put forward by one of us [2], and demonstrates several features that are unique to quantum measurement with array detectors. We demonstrate that an array detector can be used to simultaneously measure the quantum states of many different spatial modes of the same beam; here we simultaneously determine the states of two different spatial modes. Furthermore, we show that array detectors can allow for an improvement in effective detection efficiency over standard detectors when using balanced homodyne detection. This improvement comes from the fact that the local oscillator (LO) and signal fields need not be mode-matched when using array detectors. In our experiment array detection is found to be over 40 times more efficient than standard detection for measurements of a particular field mode.

The technique we use for determining the state of our field modes is quantum-state tomography (QST) [9–13]. For details about how QST is accomplished with data acquired from an array detector, see Ref. [2]; the basic idea is as follows. We wish to measure the quantum-mechanical state of a light mode that is described by a transverse spatial mode function $u_m(x)$. We will assume that the mode is one-dimensional (the case in this experiment), and that the mode function is real. The positions at the center of the pixels are

given by $x_j = j \, \delta x$, where j is an integer, and δx is the width of a given pixel. The mode function is normalized by the condition

$$\delta x \sum_j u_m^2(x_j) = 1, \qquad (1)$$

where the sum is over the pixels used in the experiment. The necessity for the measured mode function to be real is a limitation of the measurement technique. If the actual signal to be measured occupies a complex mode, the effective mode-matching efficiency when using array detection will no longer be unity; however, the efficiency will be larger than is achievable with conventional homodyne detection and a plane-wave local oscillator.

Light from the signal field of interest interferes with an LO field on a 50/50 beam splitter. The LO is a plane wave in a large-amplitude coherent state $|\beta e^{i\phi}\rangle$. The beams exiting the beam splitter are detected with array detectors. What is directly measured on each realization is a set of photoelectron numbers corresponding to each pixel. Photoelectron numbers from corresponding pixels on each detector are subtracted, yielding a set of photoelectron difference numbers that are labeled by pixel: ΔN_j. The rotated quadrature amplitude of mode m, $q_{m\phi}$, is given in terms of the difference numbers by

$$q_{m\phi} = \frac{1}{\beta} \left(\frac{D_x}{2} \right)^{1/2} \sum_j \Delta N_{j\phi} u_m(x_j), \qquad (2)$$

where D_x is the width of the measured mode [2]. The subscript ϕ indicates that the measured difference numbers and the quadrature amplitude depend on the phase of the LO.

Since we perform many measurements of $q_{m\phi}$ on an identically prepared ensemble, and for a range of phases that exceeds π, we are able to determine the quantum-mechanical state of the field corresponding to mode m using the technique of QST [12,13]. By choosing different mode functions, it is possible to use Eq. (2) to simultaneously determine the quadrature amplitudes (and hence the quantum state) of many different spatial modes for the same set of measurements. Despite the fact that the quadrature amplitudes of many modes may be measured simultaneously, it is not possible to use this technique directly to measure the joint quan-

―――――――
*Email address: beckmk@whitman.edu
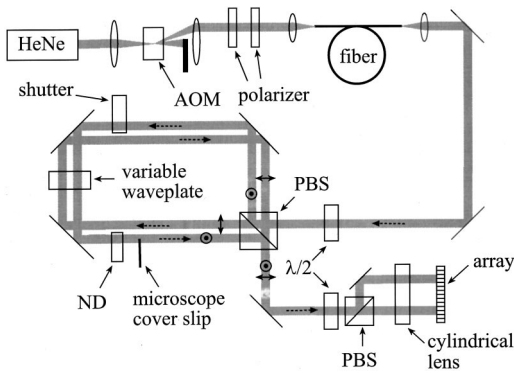
　　　63 040101-1

FIG. 1. The experimental apparatus: ND stands for neutral-density filter, PBS stands for polarizing beam splitter, and AOM stands for acousto-optic modulator. In the near common-path interferometer the polarizations and directions of the beams are indicated. The AOM, shutter, variable waveplate, and CCD array are all under computer control.

tum state of these modes. This is because all of the modes are measured with the same rotation angle ϕ; to determine the joint quantum state each mode must have its own independently adjustable phase angle [14,15].

A schematic of our experimental apparatus is shown in Fig. 1. The output from a HeNe laser is focused into an acousto-optic modulator (AOM) and then recollimated. The AOM is driven by a pulsed radio-frequency source in order to generate 10-ms-long light pulses in the first-order diffracted beam. These pulses are synchronized with the 10-ms exposure time of the CCD array. The beam then passes through a polarizer-analyzer pair that is used to adjust the light intensity, and a single-mode optical fiber that is used as a spatial filter. After emerging from the fiber, the light is collimated, passed through a $\lambda/2$ plate, and then sent to the polarizing beam splitter (PBS) that constitutes the entrance to a near common-path interferometer.

The PBS splits the incoming beam into signal and LO beams. The signal exits the beam splitter vertically polarized and travels counterclockwise around the ring, while the LO is horizontally polarized and travels clockwise. The $\lambda/2$ plate before the interferometer is used to adjust the relative intensities of these beams. The relative phase of the two beams is adjusted with a liquid-crystal variable waveplate. This waveplate has its axes aligned with the polarization axes of the beams, and it provides a phase shift to the LO that is adjustable between $0-2\pi$ as we vary the voltage applied to it.

The beams are spatially offset from each other by a few millimeters as they traverse the interferometer; this allows us to modify the signal beam without corresponding modifications to the LO. We attenuate the signal intensity by a factor of 10^3, in order to bring it down to the few photon level. We also modify the spatial structure of the signal beam in order to demonstrate that array detectors are capable of reconstructing the quantum state of a beam that has a complicated spatial structure. We do this by inserting a microscope cover slip halfway into the signal beam. The tilt angle of the cover slip is adjusted to provide a π (or an odd multiple of π) phase shift between the two halves of the beam. Near its

center, the far-field diffraction pattern of a beam modified in this way is that of a linear electric field with a π phase shift in the middle. The signal and LO return to the PBS and emerge from the interferometer spatially overlapped, but with orthogonal polarizations.

After leaving the interferometer, the beams pass through another combination of a $\lambda/2$ plate and a PBS. The $\lambda/2$ plate rotates the polarizations of the signal and LO beams so that they are at 45° with respect to the axes of the PBS so the PBS acts as a 50/50 beam splitter on which the signal and local oscillator beams interfere. The beams emerging from the PBS are focused perpendicular to the plane of Fig. 1 with a cylindrical lens, and are detected on spatially separate regions of a CCD array.

The CCD is a 100×1340 array of $20\,\mu\text{m} \times 20\,\mu\text{m}$ pixels. It has a quantum efficiency of approximately 90% at 633 nm, and is cooled to $-110\,°\text{C}$, yielding a negligible dark-count rate of less than one electron per pixel per hour. The beam is focused to a few rows in the vertical direction, so we need only read out 5 of the 100 rows of pixels. The readout rate for each exposure is approximately 15 Hz. Since we are only interested in one-dimensional information, we sum the five readings in each column to obtain an array of 1340 pixel readings: N_k, $1 \leq k \leq 1340$.

In order to determine the field quadrature amplitudes, we must calculate the difference counts for corresponding pixels in each beam, and thus need proper registration of the pixels measuring each beam. We start by finding the pixels that correspond to the center of each beam, and we refer to these pixel numbers as j_{c1} and j_{c2}. This is done by blocking the signal beam, and monitoring a plot of the difference photoelectron numbers $\Delta N_j = N_{j_{c1}+j} - N_{j_{c2}+j}$ versus pixel number for the LO only. By adjusting j_{c1} and j_{c2}, we can adjust the difference number to be approximately 0 over the majority of the beams. In the wings the difference numbers do not go to zero due to slight differences in the shapes of the two beams, but in the final analysis we do not use these pixels.

Once we have proper pixel registration, we must verify that our detector is operating at the shot-noise limit (SNL). We again block the signal, and acquire 200 shots of data for each of 30 different values of the LO intensity. We plot the variance of the difference photoelectrons for each pixel $\langle (\Delta N_j)^2 \rangle$ versus the mean of the sum of the photoelectrons $\langle S_j \rangle$, where $S_j = N_{j_{c1}+j} + N_{j_{c2}+j}$. If the detector is operating at the SNL each of these curves should be linear, with a slope equal to 1. For the 200 pixels closest to the center of the beams, we find the average slope to be 1.01 ± 0.05, indicating that our detector operates at the SNL. It is possible that differences in slopes are due to slight pixel-to-pixel variations in gain, but our statistical errors are large enough that we have chosen to use the gain specified by the manufacturer for all pixels.

We define the total difference number ΔN_T and the total sum S_T to be

$$\Delta N_T = \sum_j \Delta N_j, \quad S_T = \sum_j S_j, \quad (3)$$

where again the sums are over the pixels used in the experi-

ments. We typically use about 50 pixels close to the center of the beams, where the variation of the signal field is linear, and this defines the spatial extent of the modes we are measuring. The largest noise source in our measurements is the electronic noise associated with reading out the data from the CCD. To determine its effect, we measure the variance $\langle (\Delta N_T)^2 \rangle$ with the LO illuminating the CCD, and without illumination. With illumination, this variance is 15 dB above the variance without illumination, which is a more than adequate signal-to-noise ratio.

If the signal field is blocked (i.e., the signal mode entering the detector is in the vacuum state) then the average difference number for each pixel should be zero: $\langle \Delta N_j \rangle_{\text{vac}} = 0$, where the subscript indicates that the signal is in the vacuum state. Experimentally we find that while we can adjust the balancing of the detector (using the $\lambda/2$ plate) to yield a total difference number that averages to zero, $\langle \Delta N_T \rangle_{\text{vac}} = 0$, the average for each pixel is not necessarily zero in this case. Pixel-to-pixel variations in gain or quantum efficiency could cause this effect. However, we believe that it is due to residual high spatial frequency components that are present on the LO beams, or due to etaloning within the thin structure of the array itself, and this causes imperfect subtraction of corresponding pixels on each beam. The difference from zero is small ($\langle \Delta N_j \rangle_{\text{vac}}$ is typically less than of 1% of $\langle S_j \rangle_{\text{vac}}$), but the unbalancing of individual pixels can lead to systematic errors in QST. Furthermore, minute pointing drift of the LO beam on the array causes the balancing of individual pixels to change, consistent with the explanation that these effects arise from high spatial frequencies or etaloning. We must correct for this in our measurements, and our procedure for doing so is described below.

We collect data with the signal present by fixing the LO phase, acquiring 200 exposures, changing the LO phase, and repeating. We typically use 200 phase values evenly spaced between 0 and 2π. To correct for pixel imbalance, we numerically rebalance the array every time we adjust the LO phase. This is done by blocking the signal beam with a mechanical shutter (turning our signal mode into a vacuum), and averaging the difference numbers for each pixel to obtain $\langle \Delta N_j \rangle_{\text{vac}}$. We then unblock the signal, and subtract $\langle \Delta N_j \rangle_{\text{vac}}$ from the difference number for each pixel. Thus, in Eq. (2) we actually use the corrected difference number $\Delta N_j - \langle \Delta N_j \rangle_{\text{vac}}$ in place of ΔN_j when we calculate the quadrature amplitudes. For the amplitude of the LO coherent state we use $\beta = \langle S_T \rangle^{1/2}$, where the average is over the 200 shots for that particular phase.

In Fig. 2 we plot the corrected difference number as a function of pixel number observed across the detector for a signal field in a coherent state having a mean of approximately one photon. In Fig. 2(a) we show data collected on a single exposure, while in Fig. 2(b) the data have been averaged over 200 exposures. The two curves in each figure differ in that each curve corresponds to a different value of the LO phase; the phase difference between them is π. These curves display the spatial variation of the amplitude of the electric field of the signal, indicating a field that has a linear amplitude variation, with a π phase shift in the middle (the difference counts tend to be negative for half the beam, and
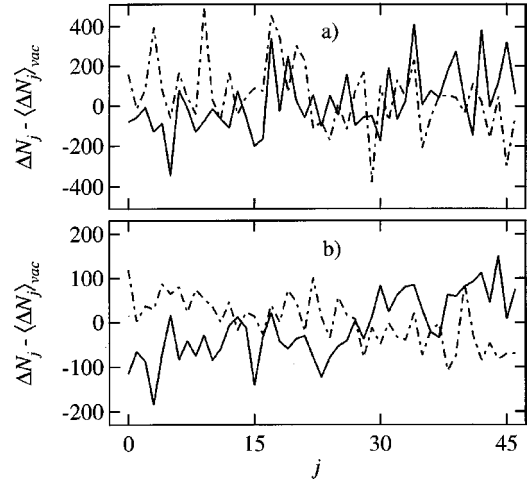

FIG. 2. The corrected difference number is plotted as a function of pixel number for a signal mode in a coherent state with a mean of approximately one photon. In (a) we show data for a single exposure, while (b) shows an average of 200 exposures. The two curves in each figure correspond to two values of the local oscillator phase that differ by π.

positive for the other half). Changing the LO phase by π causes the slope of the curves in Fig. 2 to invert (positive difference counts become negative and vice versa) as expected.

Figure 2 is a dramatic illustration of single-photon interference. While these curves contain large noise (due to the shot noise of the LO and imperfect subtraction of the vacuum difference level), they can clearly be seen to have opposite slopes. An average of one photon in the signal beam, even on single shots as shown in Fig. 2(a), can lead to macroscopic differences in the detected signal across the array.

Since the signal is linear in position, we have measured the state of the field corresponding to the properly normalized mode:

$$u_{\text{lin}}(x) = \left(\frac{12}{D_x^3} \right)^{1/2} x, \tag{4}$$

where we choose $x = 0$ to be at the center of the range of pixels we are measuring. A homodyne detector using ordinary single detectors that was detecting the same beam would not resolve the spatial differences, and would instead simply integrate over the entire detected area. This would correspond in our scheme to measuring a mode function that was constant across the array

$$u_{\text{con}}(x) = \left(\frac{1}{D_x} \right)^{1/2}. \tag{5}$$

In order to compare an array detector to a standard detector, as well as to show that array detectors can simultaneously determine the quantum states of different spatial modes, we have substituted the mode functions in Eqs. (4) and (5) separately into Eq. (2) to obtain two sets of quadrature amplitude measurements from our data. We have then used these to
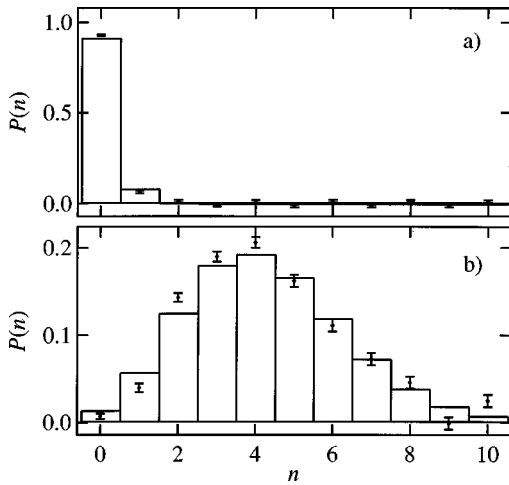
FIG. 3. Photon number distributions of the measured states corresponding to (a) $u_{con}(x)$ and (b) $u_{lin}(x)$. The points represent measured values, while the bars correspond to theoretical coherent states having the same mean number of photons. In (a) the mean photon number is 0.09, while in (b) it is 4.3.

reconstruct the quantum states of the spatial modes corresponding to Eqs. (4) and (5). The algorithm that we use for QST yields the density matrix elements of the state in the Foch state basis ρ_{mn}, as well as statistical errors associated with the matrix elements [12,13].

In Fig. 3 we show photon number distributions $P(n) = \rho_{nn}$ for the different spatial modes. Using these distributions we can calculate the mean number of photons in each mode, and we find that the constant mode contains an average of 0.09 photons, while the linear mode contains an average of 4.3 photons. The constant mode corresponds to that which would be measured by a homodyne detector that used a plane-wave local oscillator and standard single detectors. Thus, we see that such a detector would have an effective detection efficiency that is over 40 times smaller than our array detector for measuring a mode with a linear spatial variation.

Also plotted in Fig. 3 are theoretical photon number distributions for coherent states having the same mean numbers of photons. It is seen that the measured photon number distributions are nearly those of coherent states; the differences are likely due to low-frequency drift in our laser intensity. We have also used our measured values of ρ_{mn} to calculate the Wigner functions of the measured states [12,13]. The measured Wigner functions are found to agree well with the Wigner functions of coherent states having the same mean amplitude.

In conclusion, we have experimentally demonstrated the use of an array detector to perform state measurements on an optical beam having a nontrivial spatial distribution. Array detection has an advantage over standard detection for this task because it allows for the simultaneous determination of the quantum states of multiple spatial modes in the beam, and it also allows for greater effective detection efficiency.

[1] M. G. Raymer, J. Cooper, and M. Beck, Phys. Rev. A **48**, 4617 (1993).

[2] M. Beck, Phys. Rev. Lett. **84**, 5748 (2000).

[3] C. Iaconis, E. Mukamel, and I. A. Walmsley, J. Opt. B: Quantum Semiclassical Opt. **2**, 510 (2000).

[4] M. I. Kolobov, Rev. Mod. Phys. **71**, 1539 (1999).

[5] A. Gatti, E. Brambilla, L. A. Lugiato, and M. I. Kolobov, Phys. Rev. Lett. **83**, 1763 (1999).

[6] A. Gatti, K. I. Petsas, I. Marzoli, and L. A. Lugiato, Opt. Commun. **179**, 591 (2000).

[7] M. Marable, S.-K. Choi, and P. Kumar, Opt. Express **2**, 84 (1998).

[8] S.-K. Choi, M. Vasilyev, and P. Kumar, Phys. Rev. Lett. **83**, 1938 (1999).

[9] K. Vogel and H. Risken, Phys. Rev. A **40**, 2847 (1989).

[10] D. T. Smithey, M. Beck, M. G. Raymer, and A. Faridani, Phys. Rev. Lett. **70**, 1244 (1993).

[11] D. T. Smithey, M. Beck, J. Cooper, M. G. Raymer, and A. Faridani, Phys. Scr. **T48**, 1514 (1993).

[12] U. Leonhardt, *Measuring the Quantum State of Light* (Cambridge University Press, Cambridge, England, 1997).

[13] G. M. D'Ariano, in *Quantum Optics and the Spectroscopy of Solids*, edited by T. Hakioglu and A. S. Shumovsky (Kluwer, Dordrecht, 1997), p. 139.

[14] H. Kuhn, D.-G. Welsch, and W. Vogel, Phys. Rev. A **51**, 4240 (1995).

[15] M. G. Raymer, D. F. McAlister, and U. Leonhardt, Phys. Rev. A **54**, 2397 (1996).